FLOW INDUCED VIBRATIONS IN METAL BELLOWS

By

H. J. Bandgren*

SUMMARY

This paper summarizes the results of an experimental and analytical study of flow induced vibration of metal bellows. The results of numerous laboratory experiments have confirmed that vortex shedding from the tips of the bellows convolutions is the fluid excitation mechanism. When the frequency of the vortex shedding coincides with one of the natural longitudinal resonant frequencies of the free bellows or braided hose, a strong bellows vibration may exist.

A semiempirical method of estimating the flow induced dynamic stresses in a bellows for a given set of flow conditions has been formulated. Design methods for eliminating or minimizing the effects of flow induced vibration in bellows systems have been developed and experimentally verified.

The criteria presented in this paper were used to assess all of the metal bellows in the Saturn/Apollo launch vehicle system to determine if flow induced vibration problems existed. Corrective action was implemented where necessary by the installation of flow liners or the addition of damping to the bellows system.

INTRODUCTION

During the flight of the second Saturn V space vehicle, AS-502, one of the J-2 engines on the second stage malfunctioned causing the engine to shut down early. During the same flight the J-2 engine on the third stage failed to restart in earth orbit. More recently, during static firings of the S-IVB flight stages for AS-508 and AS-509, the LH_2 propellant delivery lines developed leaks. All of these anomalies were determined to be the result of flow induced vibration fatigue failures of the metal bellows.

This paper describes the results of an analytical and experimental study of flow induced vibrations in metal bellows. A number of significant findings have been made throughout this study and are discussed in detail in the paper; these are listed below:

1. The fluid-elastic mechanism causing bellows flow excitation (vortex shedding) has been observed in the laboratory and is discussed.

2. A semiempirical method for estimating the flow induced dynamic stresses in a bellows for a given set of flow conditions is described.

3. Methods of eliminating or minimizing flow induced dynamic stresses are presented. Internal flow liners and various bellows external damping devices have been tried as a means of suppressing the bellows flow induced vibrations.

VORTEX SHEDDING FROM BELLOWS CONVOLUTIONS, THE FLOW EXCITATION MECHANISM

It is documented in the literature that when there is fluid flow over a cylinder, as shown in Figure 1, with a sufficiently high Reynolds number, a succession of alternately shed vortices will occur in the near wake region of the cylinder. Over a Reynolds number range of from 300 to 300 000, the frequency of the vortex shedding is related to the Strouhal number (S), flow velocity (V), and the diameter (D) of the cylinder as shown in Figure 1. This same phenomenon has been shown to occur when fluid flows through a bellows with open convolutes, as depicted at the bottom of Figure 1. The length quantity is σ, the width of the convolute.

When the vortex shedding frequency of the bellows coincides with one of the longitudinal resonant frequencies of the bellows, a strong bellows vibration may result. To verify this, the response characteristics of numerous bellows were studied in the flow facility. Figure 2 shows the flow induced dynamic stress at the tip of the convolute for a typical free bellows. This is a single ply bellows with an inside diameter of 5.08 cm (2.0 in.) and a convolute width of 0.3175 cm (0.125 in.). A graph of root

*This study was performed in conjunction with Southwest Research Institute under contract NAS8-21133 with Dr. C. R. Gerlach as the principal investigator.

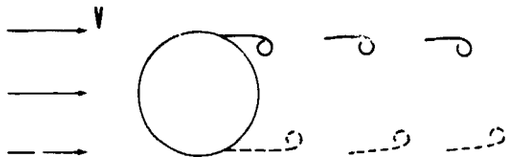

$f = SV/D = 0.2\ V/D$

VORTEX SHEDDING FROM CYLINDER

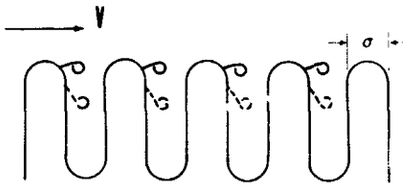

$f = SV/\sigma = 0.2\ V/\sigma$

VORTEX SHEDDING FROM BELLOWS CONVOLUTIONS

Figure 1. Vortex shedding process.

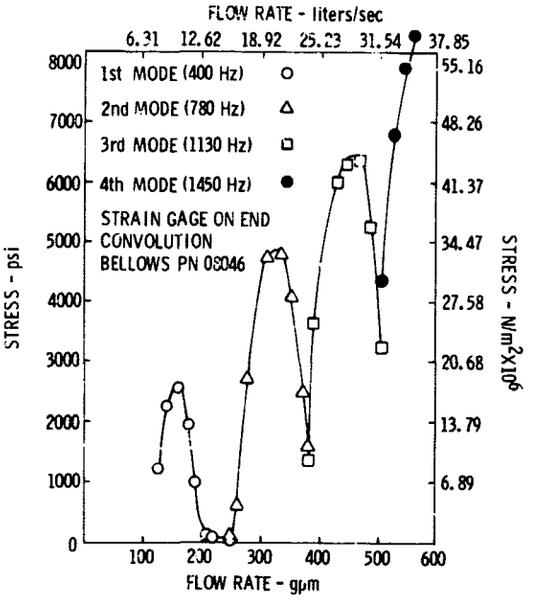

Figure 2. Bellows stress as a function of flow rate for four flow excited modes of vibration.

mean square stress at the tip of the end convolution is plotted against flow rate in liters/sec (gallons per minute are also shown). As the flow rate increased, a succession of bellows modes were excited. Before the bellows was installed in the flow facility, it was filled with water, capped off, and fixtured on an electrodynamic shaker to identify its longitudinal natural frequencies. These were 400 Hz for the first mode, 780 Hz for the second mode, 1130 Hz for the third mode, and 1450 Hz for the fourth mode. The significance here is that the flow rate corresponding to each of the stress build-ups shown in Figure 2 resulted in a particular vortex shedding frequency that coincided with one of the longitudinal resonant frequencies of the bellows when a Strouhal number of approximately 0.2 was used in the calculation for the vortex shedding frequency. Also, the dynamic stress increased as the mode number increased, because the vortex shedding forces are proportional to the free-stream stagnation pressure, $\frac{1}{2}\rho V^2$ (where ρ is the fluid mass density).

The type of longitudinal resonant modes that are excited in a free bellows are shown in Figure 3. These resonant modes are sometimes referred to as the accordion modes. For the first four natural modes of the previous bellows, axial displacement is plotted on the ordinate as a function of position along the bellows on the abscissa. The first natural mode is 400 Hz. There are nodes at the ends of the bellows, and all of the convolutions are moving in phase with the maximum motion at the center of the bellows. The second mode is 780 Hz. The nodes are at the center and end points of the bellows, and the maximum motion is at the quarter points 180 degrees out of phase. See Figure 3 for a description of the third and fourth modes.

A bellows vibrating in one of its accordion modes is better represented by a lumped parameter system than by a continuous system. The mechanical model shown at the bottom of Figure 3 was found to give quite adequate predictions of the longitudinal bellows frequencies. The model consists of a series of equal

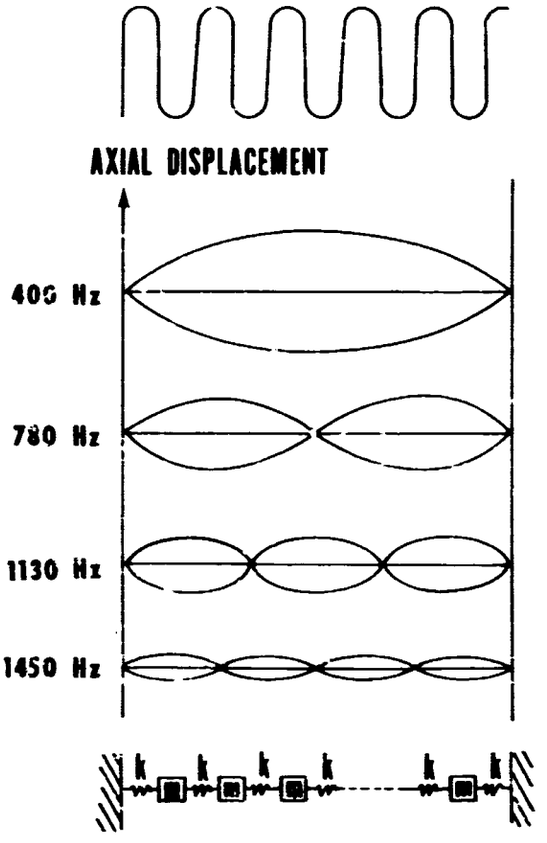

Figure 3. Observed bellows longitudinal vibration mode shapes.

springs (k) and masses (m) fixed at the ends. The individual springs can be determined from the axial spring rate of the bellows; the masses can be determined from the total mass of the bellows convolutions plus the mass of the fluid trapped in the root of the convolutes. The mass and flexibility matrices can be determined from the model, and any standard eigenunction routine will provide the resonant frequencies and mode shapes.

For a braided hose the type of modes that are excited by the vortex shedding forces are shown in Figure 4. The adjacent crowns of the convolutes are fixed by the wire braid, and a simple cantilever mode of the individual roots of the convolutes is excited. These are sometimes referred to as reed modes, and the spring mass system is a simple one as shown at the bottom of Figure 4.

Experimental stroboscopic observations have been used to verify that these are the longitudinal

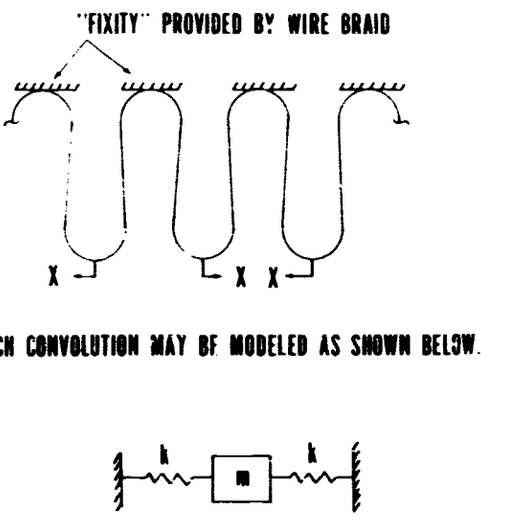

Figure 4. Metal hose flow excited vibration mode.

bellows modes that are excited by the vortex shedding forces. To experimentally verify that vortex shedding is the mechanism that is exciting the longitudinal modes of the bellows, a model consisting of a two-dimensional clear plastic channel containing a short section of convoluted metal was constructed, as shown in Figure 5, and placed in the flow facility. As in an actual bellows, the convolution tips are exposed to the fluid flow. When water is passed through the channel at the proper flow velocity, the convolutions are flow excited. By injecting ink upstream from the convoluted segment and by slowing down the motion with the aid of a strobe light, the vortex shedding process was readily visualized, and motion pictures were taken.

Figure 6 shows the sequence of fluid and convolution events that were observed in a frame-by-frame examination of the motion pictures. Note that the mode of vibration of the segment is one where each convolution moves out of phase with the adjacent convolutions. The vortex shedding process on the vibrating convolution segment, as shown in Figure 6, occurs as follows:

1. Position I — A large vortex c has formed between convolutions 1 and 2. A small vortex b is beginning to form on the downstream side of convolution 2. A large vortex a is moving across the tip of convolution 3; its origin will become apparent later.

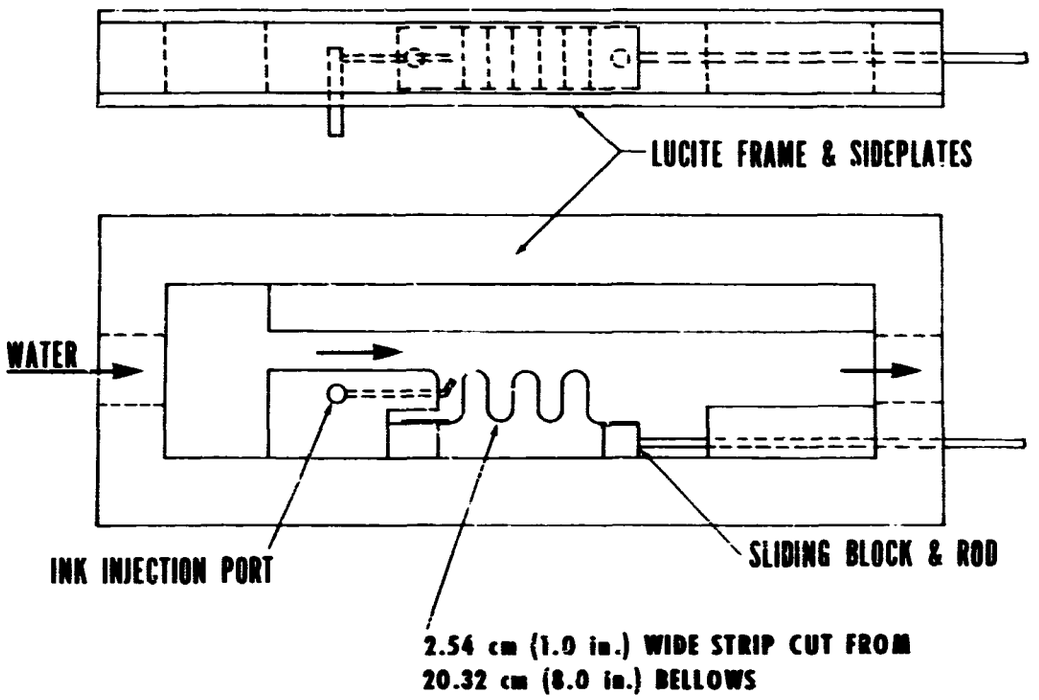

Figure 5. Two-dimensional bellows flow visualization model.

2. Position II — Vortex c has been pushed downstream by the pinching action of convolutions 1 and 2. Vortex b is gaining in strength on the downstream side of convolution 2. Vortex a is propagating downstream.

3. Position III — The space between convolutions 1 and 2 has opened up causing the fluid to be drawn in, and vortex d is beginning to form on the downstream side of convolution 1. Vortex c has been swept over the top of convolution 2 with the timing being about right to combine with vortex b, forming the larger vortex b + c.

4. Position IV — Vortex d is gaining in strength on the downstream side of convolution 1. Vortex b + c is being pushed out into the fluid stream by the "pinching" action of convolutions 2 and 3.

5. Position V — This is the same as position I completing one cycle of the vortex shedding process. Note that vortex a in position I is the combination of two vortices, as is b + c in position V.

SEMIEMPIRICAL METHOD FOR ESTIMATING FLOW INDUCED DYNAMIC STRESSES IN METAL BELLOWS

The previous discussion has been directed to the problem of when and how a bellows can be flow excited. The coincidence of the longitudinal resonant frequencies of a bellows with the vortex shedding frequency does not indicate the severeness of the vibration. During this study, an attempt has been made to predict vibration amplitudes and corresponding stress levels in a bellows for a given set of flow conditions.

Figure 7 shows the fluid and structural dynamics involved in bellows flow excitation. The process of periodic vortex formation and shedding causes a corresponding periodic pressure to be exerted on the bellows convolutions. The amplitude of this alternating pressure is proportional to the free-stream

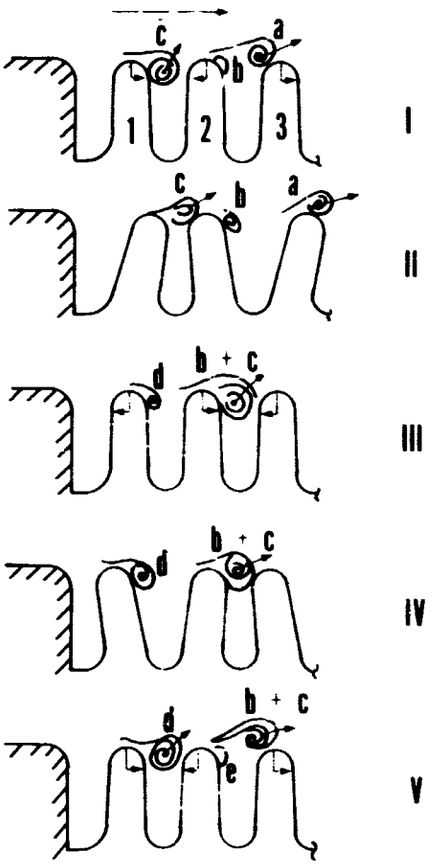

Figure 6. Sequence of coupled fluid-convolution events observed with two-dimensional bellows flow visualization model.

stagnation pressure $\frac{1}{2}\rho V^2$. So far as the bellows structure is concerned, the effect of this alternating pressure may be considered as a net force applied at the tip of each convolution. This force is called the vortex shedding force. The semiempirical equations for the vortex force, the convolution displacement, and the resulting stress at the tip of the convolution are shown in Figure 7.

Figure 8 shows the model that was used to determine the value of the vortex force coefficient C_F. A single bellows convolution was simulated in this test by a flexible steel ring clamped in a special housing between a pair of exciter coils. A displacement probe was built into the apparatus to allow ring vibration amplitudes to be monitored. The convolution vibration test model was placed in

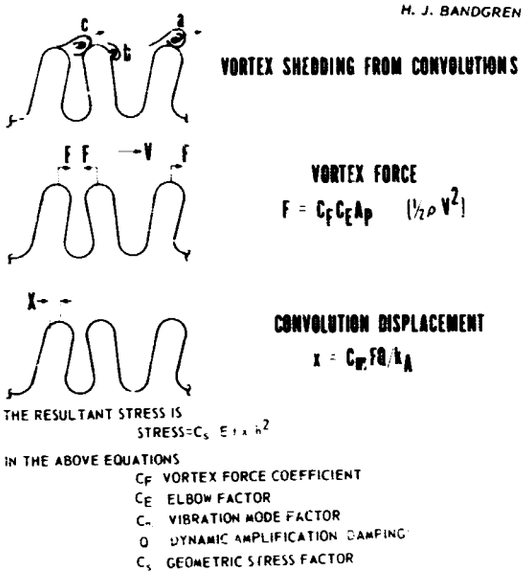

Figure 7. Illustration of stress resulting from vortex force.

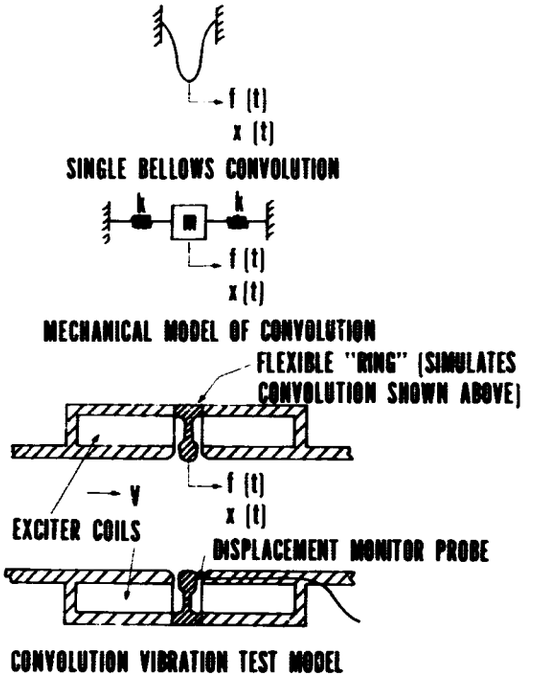

Figure 8. Diagram of convolution vibration test model and equivalent bellows and mechanical model representations.

the flow facility, and the vibratory response of the ring in water was determined with the excitation provided by the exciter coils. Next, the frequency response of the ring was determined with the fluid flow providing the excitation. Finally, a static force versus deflection calibration was made on the ring. The data from these tests were used as follows:

1. Vibration amplitude as a function of fluid velocity was converted to an apparent force using the data from the force-deflection calibration.

2. This apparent force was converted to a true vortex force by dividing it by the dynamic amplification factor Q, obtained from the forced vibration test in water.

3. The vortex force coefficient C_F was then determined from the equation for the vortex force shown in Figure 7.

Vortex coefficient data were obtained in this manner for several convolution geometries. They were also obtained from numerous tests on real bellows. The results of these tests are summarized in Figure 9. The vortex force coefficient C_F is plotted on the ordinate as a function of the ratio of pitch to convolute tip width on the abscissa. Notice the great reduction in the force coefficient as the convolution pitch is opened.

The next factor in the vortex force equation shown in Figure 7 is the elbow coefficient C_E. The

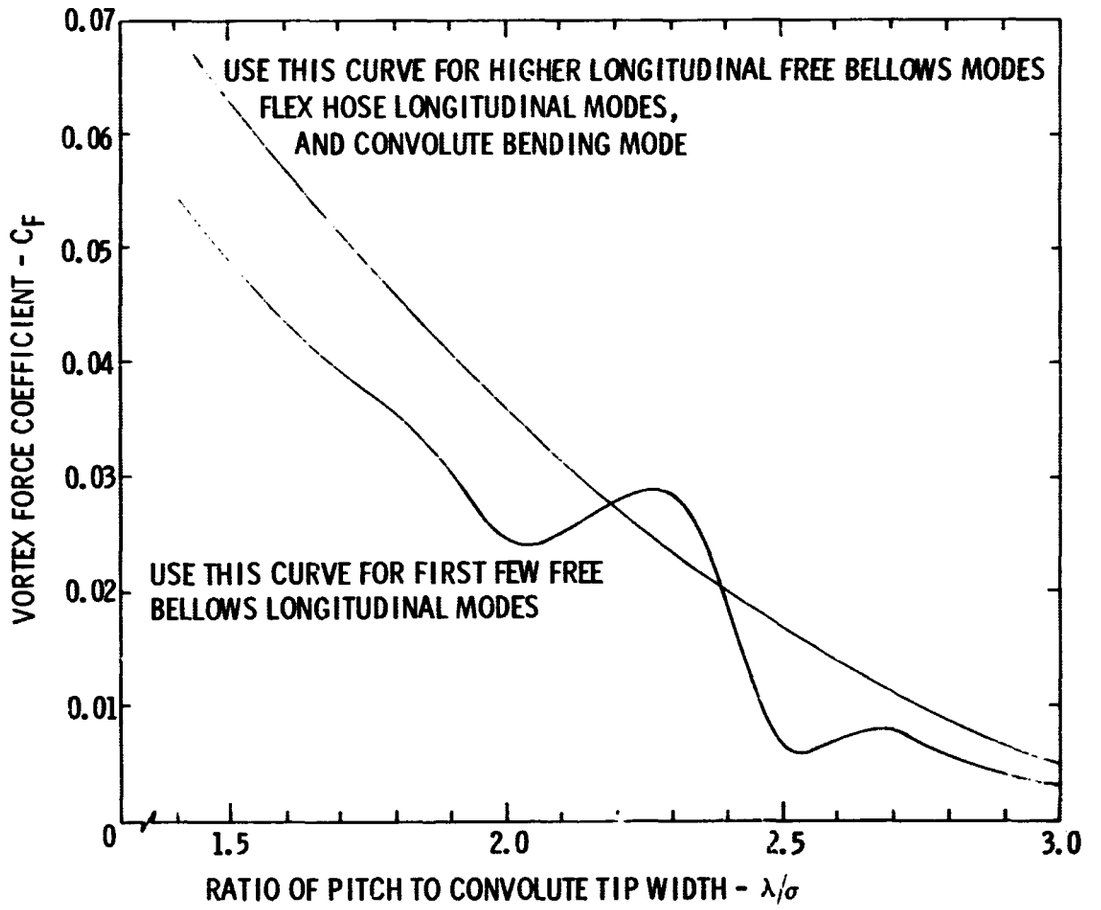

Figure 9. Summary of bellows vortex force coefficient experimental data.

presence of an elbow upstream from a bellows causes excessive flow induced dynamic stresses because of the increased turbulence. There is little quantitative data available on this effect, but the available data suggest correcting the vortex shedding force upward by a factor of 2.0 to account for the presence of an upstream elbow.

A_p is the projected area of the convolution and can be approximated by the product of the mean circumference and the height of the convolute. The final quantity in the vortex force equation is the free stream stagnation pressure $\frac{1}{2}\rho V^2$.

The convolution displacement resulting from the vortex force is shown in the second equation of Figure 7. The vibration mode factor C_m relates displacement and force for a given resonant condition. The following assumptions were made in the derivation of the vibration mode factor:

1. The shape of the longitudinal bellows modes is intermediate between a linear and sinusoidal form.

2. The maximum deflection for a given mode is equal to the static deflection times Q, the dynamic amplification factor.

3. The maximum stress point for a given vibration mode occurs at the convolution with the maximum relative displacement. Generally, this is the end convolution for each half-wave mode shape.

The first assumption implies that the mode shape over the first quarter wavelength is

$$x = \frac{x_o}{2}\left[\left(\frac{N}{\ell}\right)Y + \sin\left(\frac{N\pi Y}{\ell}\right)\right] , \qquad (1)$$

where x denotes the axial absolute displacement of a given point along the bellows defined by the axial position coordinate Y, N is the mode number, and ℓ is the length of the bellows.

The second assumption implies that the maximum absolute displacement x_o is

$$x_o = \frac{FQ}{4NK_A} , \qquad (2)$$

where F is the vortex shedding force, Q is the dynamic amplification factor, and K_A is the axial spring rate of the bellows.

From the third assumption, the point of maximum relative displacement x_{mr} for a given bellows, and a given mode of vibration, occurs at a point where $Y = \ell/2N_C$. Therefore, from equation (1)

$$x_{mr} = \frac{x_o}{2}\left[\frac{N}{N_C} + \sin\left(\frac{\pi}{2}\frac{N}{N_C}\right)\right] . \qquad (3)$$

Combining equations (2) and (3) yields

$$x_{mr} = \frac{FQ}{8NK_A}\left[\frac{N}{N_C} + \sin\left(\frac{\pi}{2}\frac{N}{N_C}\right)\right] , \qquad (4)$$

and by comparison with the equation for the convolution displacement in Figure 7, the vibration mode factor C_m is

$$C_m = \frac{1}{8N}\left[\frac{N}{N_C} + \sin\left(\frac{\pi}{2}\frac{N}{N_C}\right)\right] \qquad (5)$$

Returning now to the equation for the convolution displacement shown in Figure 7, the next factor is the vortex shedding force F that has been discussed and then the dynamic amplification factor Q, a measure of damping. Physically, Q represents the ratio of the vibration amplitude at resonance to the vibration amplitude in the limits of zero frequency. It also can be expressed as the resonant frequency divided by the frequency bandwidth at the half-power points for a given resonant buildup. Because Q is so important in the prediction of bellows flow induced dynamic stresses, a large number of tests were performed from which Q values could be obtained. Each bellows tested was installed in a special fixture that rigidly connected the end flanges. This was to insure that the vibration modes excited were the same as those excited by the vortex shedding forces. The bellows were then excited with an electrodynamic shaker with the output strain at the tip of the convolutes measured to obtain Q values. Some observations noted during this testing were as follows:

1. As the strain was increased, the damping increased and lowered the Q values.

2. Increasing the number of plies in a bellows increases the damping significantly.

3. Going from a low pressure gas to a high pressure gas or from a light liquid to a dense liquid increases the damping.

Some typical Q values as a function of number of plies and flow media are:

No. Plies	Medium	Q Range
1	Air or low pressure gases	150 to 200
1	High pressure gases or light liquids	100 to 150
1	Heavy liquids	50 to 100
2	Gases	40 to 50
2	Liquids	30 to 40
3	All	20 to 40

The last factor in the convolution displacement equation is K_A the axial spring rate of the bellows. The most accurate method for determining K_A is from load deflection tests in the laboratory. Probably the most accurate analytical method for determining bellows spring rate was developed by the Battelle Memorial Institute. This is a computerized method that provides for both linear and nonlinear elastic deformations. Most noncomputerized techniques use equations similar to those developed by F. Salzmann.

The last equation in Figure 7 is for the resultant stress at the tip of the bellows convolution. The stress is related to Young's modulus (E) and ply thickness (t) of the bellows material, and the height (h) and deflection of the convolute by a geometric stress factor C_s. Here again, the Battelle Memorial Institute has obtained very good agreement between theoretical and experimental methods using a computer solution for the stress deflection relationship. However, the Salzmann equations for determining the stress in a bellows for a given convolution displacement compare favorably with the experimental test results.

METHODS OF ELIMINATING OR MINIMIZING FLOW INDUCED DYNAMIC STRESSES

The mechanism by which metal bellows are excited by flow induced vibration and a semiempirical method of estimating the resulting stresses have been discussed. The question now is: how can these dynamic stresses be eliminated or minimized? The installation of an internal flow liner in a bellows will eliminate flow induced dynamic stresses, when the liner design covers all of the active convolutions. The cone shape of most liners allows angular movement of the bellows but produces a constriction, resulting in unwanted pressure drops.

A method for reducing the flow stresses in a bellows is to add damping to the bellows structure. This can be accomplished by the following methods:

1. Increasing the number of plies of the bellows.

2. Filling the convolutions with some viscoelastic material such as rubber or 3M strip-caulk.

3. Placing a soft metal spring in each of the bellows convolutions.

4. Tightly wrapping the exterior of the bellows with wire screen.

Experimental results show all of these methods afford a considerable amount of damping.

CONCLUSIONS

An examination of test results of flow induced vibrations of numerous bellows confirmed that vortex shedding from the bellows convolutions is the excitation mechanism. When the vortex shedding frequency coincides with one of the natural resonant modes of the bellows, a strong vibration may exist.

Tests results compare favorably with the semiempirical method presented in this paper for predicting the flow induced dynamic stresses. They also confirm that the external damping devices suppress flow induced vibrations of bellows.

The results of this study were used to assess all of the bellows on the Saturn/Apollo launch vehicle system to determine flow induced vibration susceptibility and to provide guidelines for all necessary corrective action.

BIBLIOGRAPHY

Gerlach, C. R.: Study of Minimum Pressure Loss in High Velocity Duct Systems. Quarterly Report No. 4, Contract NAS8-21133, Southwest Research Institute, May 1968.

Gerlach, C. R.: Study of Minimum Pressure Loss in High Velocity Duct Systems. Quarterly Report No. 5, Contract NAS8-21133, Southwest Research Institute, August 1968.

Aerospace Recommended Practice (ARP) No. 735. Society of Automative Engineers Publications, 1966.

Gerlach, C. R.; and Schroder, E. C.: Study of Minimum Pressure Loss in High Velocity Duct Systems. Interim Technical Report No. 1, Contract NAS8-21133, Southwest Research Institute, July 1969.

Trainer, T. M.; Hulbert, L. E.; Lestingi, J. F.; Keith, R. E.; et al: Technical Report No. AFRPL-TR-68-22. Battelle Memorial Institute, March 1968.